

# Factors governing energy relaxation in disordered charge and spin density waves

R. Mélin<sup>(1)\*</sup>, K. Biljaković<sup>(2)</sup> and J.C. Lasjaunias<sup>(1)</sup>

<sup>(1)</sup> Centre de Recherches sur les Très Basses Températures (CRTBT)<sup>†</sup>,  
Boîte Postale 166, F-38042 Grenoble Cedex 9, France

<sup>(2)</sup> Institute of Physics, Hr-10 001 Zagreb, P.O. Box 304, Croatia

To explain heat relaxation experiments we investigate collective effects in disordered charge and spin density waves (CDWs and SDWs). We discuss the models in the classical and quantum limits that contribute to two distinct contribution to the specific heat (a  $C_v \sim T^{-2}$  contribution and a  $C_v \sim T^\alpha$  contribution respectively), with two different types of disorder (strong pinning versus substitutional impurities). From the calculation of the two level system energy splitting distribution in the classical limit we find no slow relaxation in the commensurate case and a broad spectrum of relaxation times in the incommensurate case. In the commensurate case quantum effects restore a non vanishing energy relaxation, and generate stronger disorder effects in incommensurate systems. For substitutional disorder we obtain Friedel oscillations of bound states close to the Fermi energy. With negligible interchain couplings this explains the power-law specific heat  $C_v \sim T^\alpha$  observed in experiments on CDWs and SDWs combined to the power-law susceptibility  $\chi(T) \sim T^{-1+\alpha}$  observed in the CDW o-TaS<sub>3</sub>.

PACS numbers: Pacs numbers

## I. INTRODUCTION

There exist many examples of systems showing slow relaxation and ageing: spin glasses<sup>1,2</sup>, disordered dielectrics<sup>3,4,5</sup>, supercooled liquids<sup>6</sup>, etc ... Charge density waves (CDWs) and spin density waves (SDWs)<sup>7,8,9,11</sup> show “interrupted ageing”<sup>12</sup>, meaning that there exists an upper bound  $\tau_{\max}$  to the relaxation times. The protocol of ageing experiments in CDWs and SDWs is the following: the system is equilibrated at the temperature  $T$  (one waits for a time longer than  $\tau_{\max}$ ). At time  $t = 0$  the temperature is changed from  $T$  to  $T + \Delta T$  where  $\Delta T > 0$  is very small compared to  $T$ . The temperature is kept constant until the waiting time  $t_w$  where it is brought back to  $T$ . The heat flows between the CDW or SDW sample and the cold source are recorded as a function of time. Ageing in the thermal response takes place even for very small values of  $\Delta T$ . It is thus not unreasonable to suppose that the correlation length does not evolve in time and remains approximately equal to the zero temperature correlation length. This behavior can be contrasted with usual ageing experiments where large temperature variations are applied so that the correlation length is a function of time.

In a recent work<sup>13</sup> we applied the idea of dynamical renormalization group<sup>14,15</sup> to calculate the spectrum of relaxation times of a model of disordered CDW or SDW<sup>16,17,18,19,20,21,22,23</sup>, including interactions among solitons. In this approach we suppose that the CDW or SDW undergoes a quench from high temperature so that

there exists a correlation length  $\xi(t)$  that increases with time and saturates to a finite value in the large time limit. We also proposed a phenomenological Random Energy Model-like (REM-like)<sup>12,24</sup> trap model that was able to fit the long time tail of the relaxation spectrum. This approach was able to account for a broad spectrum of relaxation times but several points that we want to clarify here remained unexplained.

The main message of the following article is that there exist two limiting cases relevant to experiments in disordered CDWs and SDWs: the “classical” limit where the CDW or SDW is viewed as a classical elastic medium with soliton-like excitations generated by strong pinning impurities distributed at random, and the “quantum” limit where solitons due to substitutional disorder interact quantum mechanically by excitations of the gaped background. The necessity of invoking two effects arises from the experimental observation that the low temperature out-of-equilibrium specific heat can be decomposed into three contributions: (i) the  $C_v \sim 1/T^2$  tail of a Shottky anomaly at very low temperature (typically for  $T \lesssim 100 \div 300$  mK; the upper bound depends on the amplitude of the  $1/T^2$  contribution); (ii) a  $C_v \sim T^\alpha$  power-law susceptibility with  $\alpha \simeq 0.3 \div 1.2$  at intermediate temperatures ( $0.1 \lesssim T \lesssim 1$  K); and (iii) the “trivial” contribution of phonons  $C_v \sim T^3$  at high temperature ( $T \gtrsim 1$  K). The contribution (i) is interpreted in terms of two-level systems due to strong pinning impurities. The contribution (ii) is interpreted as midgap states interacting through Friedel oscillations. Friedel oscillations of a single impurity were probed directly by -ray diffraction experiments in Ref. 25. Another evidence in favor of the coexistence of strong pinning and substitutional impurities is that the CDW compound o-TaS<sub>3</sub> can be doped by Nb, a substitutional impurity, which changes only the amplitude of the  $C_v \sim T^\alpha$  contribution, but leaves un-

\*E-mail: melin@grenoble.cnrs.fr

<sup>†</sup>U.P.R. 5001 du CNRS, Laboratoire conventionné avec l’Université Joseph Fourier

changed the  $Cv \sim 1/T^2$  contribution<sup>26</sup>.

The classical limit is based on a soliton energy landscape as a function of a “coordinate”  $X$ , valid for an arbitrary number of impurities contributing to pinning the soliton. Deviations from commensurability for a single impurity<sup>22</sup> constitutes a first source of disorder. Disorder comes also into play through a fluctuating number of strong pinning impurities contributing to pinning a given soliton-like deformation of the CDW or SDW. The number  $N_{\text{imp}}$  of impurities within a distance equal to the width  $\xi$  of the soliton is given by the binomial distribution. The average number of impurities is  $\overline{N}_{\text{imp}} = x\xi$ , with  $x$  the concentration of impurities. The root mean square  $\sigma = \sqrt{\overline{N}_{\text{imp}}^2 - \overline{N}_{\text{imp}}^2} = \sqrt{\xi x(1-x)}$  is larger than  $\overline{N}_{\text{imp}}$  if  $x\xi < 1$ . This is why we cannot neglect the fluctuations in  $N_{\text{imp}}$ .

One of our motivations is a recent experimental work<sup>27</sup> in which it was shown that relaxation in the commensurate organic spin-Peierls compound  $(\text{TMTTF})_2\text{PF}_6$  was heterogenous, qualitatively different from homogeneous relaxation in the organic incommensurate SDW  $(\text{TMTSF})_2\text{PF}_6$ . In the commensurate case the spectrum of relaxation times  $P_{t_w}(\ln \tau)$  is bimodal, with two time scales  $\ln \tau_1 < \ln \tau_2$  that are almost independent on  $t_w$ . For short waiting times most of the weight is on  $\ln \tau_1$  whereas for large waiting times the weight is transferred to the mode at  $\tau_2$ . By contrast in the incommensurate case the average of the logarithm of the relaxation time increases with  $\ln t_w$  and the width of the spectrum also increases with  $\ln t_w$ . In the following we propose an explanation to the difference between the commensurate and incommensurate cases, based on a symmetry of the energy landscape in the commensurate case. We show also the necessity of describing impurities on the basis of a quantum mechanical model.

The commensurate organic spin-Peierls compound  $(\text{TMTTF})_2\text{PF}_6$  showing slow relaxation contrasts with the inorganic spin-Peierls compound  $\text{Cu}_{1-x}\text{Zn}_x\text{GeO}_3$ <sup>28,29,30,31</sup> showing antiferromagnetic ordering. The difference probably lies in the different nature of disorder. Substitutional disorder relevant to  $\text{Cu}_{1-x}\text{Zn}_x\text{GeO}_3$  is qualitatively different from strong pinning impurities in CDWs and SDWs. For substitutional disorder we find interactions among solitons due to Friedel oscillations. For weak interchain interactions we obtain similarly to Ref. 32 a power-law specific heat  $C_v(T) \sim T^\alpha$  and a susceptibility  $\chi(T) \sim T^{-1+\alpha}$  in agreement with existing experiments on the SDW o-TaS<sub>3</sub><sup>26</sup>.

The article is organized as follows. In section II we investigate a classical model of collective effects in a disordered CDW. Quantum effects are investigated in section III. Final remarks are given in section IV.

## II. CLASSICAL LIMIT (STRONG PINNING IMPURITIES)

### A. Existing results

#### 1. One impurity

Let us start with a classical model of disordered CDW. The Hamiltonian is given by<sup>16,17,18,19,20,21,22,23</sup>

$$\mathcal{H} = w \int dx [1 - \cos \varphi(x)] + \frac{\hbar v_F}{4\pi} \int dx \left( \frac{\partial \varphi(x)}{\partial x} \right)^2 (1) \\ - \sum_i V_i [1 - \cos(Qx_i + \varphi(x_i))],$$

where the sum in the last term runs over all impurities, distributed at random.  $w$  is the interchain interaction,  $v_F$  the Fermi velocity and  $V_i$  the pinning potential associated to the impurity at position  $x_i$  and  $Q$  is the wave vector of the CDW. Minimizing the energy with respect to  $\varphi(x)$  leads to the exact expression of the phase profile of the soliton associated to an impurity located at position  $x_1$  with a pinning potential  $V_1$ :

$$\tan \left( \frac{\varphi(x)}{4} \right) = \tan \left( \frac{\psi}{4} \right) \exp \left( -\frac{|x - x_1|}{\xi} \right), \quad (2)$$

where  $\psi$  is such that

$$\sin \left( \frac{\psi}{2} \right) = \frac{\pi V_1 \xi}{2 \hbar v_F} \sin(\alpha_1 + \psi), \quad (3)$$

with  $\alpha_1 = Qx_1$ . The soliton-like solution has a decay length given by  $\xi = \sqrt{\hbar v_F / 2\pi w}$ . To simplify the semantics we call Eq. (2) a “soliton” even though strictly speaking it corresponds to a dipole made of two solitons with opposite charges.

#### 2. A finite concentration of impurities

We suppose that there exist solitons of width  $l$  and decay length  $\xi$  separated by regions where  $\varphi(x) \simeq 0$  (see Fig. 1) and that several impurities can contribute to pinning a given soliton. The width  $l$  is the length scale over which  $\varphi(x)$  can be approximated as constant in the middle of the soliton whereas the decay length  $\xi$  is the length scale over which  $\varphi(x)$  relaxes to zero. The two length scales  $\xi$  and  $l$  are comparable if  $x\xi$  is of order unity. We note  $N_{\text{imp}}$  the number of impurities within the width  $l$  of a given soliton. In the binomial model that we consider below the concentration of impurities  $x$  is fixed, the correlation length  $\xi$  is fixed but  $N_{\text{imp}}$  is fluctuating from one soliton to the other. The probability to find  $N_{\text{imp}}$  solitons within the decay length  $\xi$  is

$$\mathcal{P}(N_{\text{imp}}) = \frac{N_{\text{imp}}!}{\xi!(\xi - N_{\text{imp}})!} x^{N_{\text{imp}}} (1 - x)^{\xi - N_{\text{imp}}}. \quad (4)$$

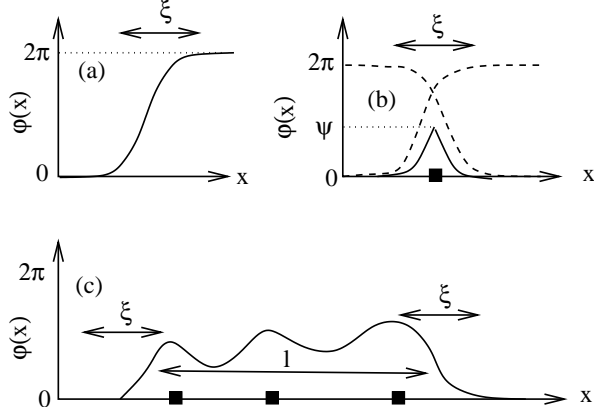


FIG. 1: Schematic representation of the spatial variation of the phase  $\varphi(x)$  along a chain. (a) A  $2\pi$  soliton varying over a length  $\xi$ . (b) A dipole<sup>21</sup> (superposition of a  $2\pi$ -soliton and a  $2\pi$ -anti soliton) varying over a length  $\xi$  generated by one strong pinning impurity. (c) A soliton generated by the clustering of three strong pinning impurities at a distance much smaller than the average distance between impurities. The phase decays over a length  $\xi$  whereas the soliton has a width  $l$ . The square boxes represent the impurities.

The binomial distribution is close to a Gaussian for  $x\xi \gtrsim 1$  but deviates strongly from the Gaussian for  $x\xi \lesssim 1$ . The condition at which solitons do not proliferate can be obtained from a different model where two neighboring impurities belong to the same cluster if their distance is smaller than  $\xi$ . The probability to find  $N_{\text{imp}} \geq 1$  solitons in a given cluster follows the exponential distribution

$$\mathcal{P}(N_{\text{imp}}) = \exp(-x\xi) [1 - \exp(-x\xi)]^{N_{\text{imp}}-1}, \quad (5)$$

where the average number of impurities within the width  $l$  of a soliton is equal to  $\exp(x\xi)$ . Solitons do not proliferate if  $x\xi \lesssim 1$ .

A soliton profile generalizing Ref. 13 is given by

$$\tan\left(\frac{\varphi(x)}{4}\right) = \sum_{i=1}^{N_{\text{imp}}} \tan\left(\frac{\psi_i}{4}\right) \exp\left(-\frac{|x-x_i|}{\xi}\right), \quad (6)$$

where  $\psi_i$  are variational parameters determined from minimizing the energy. Eq. (6) is obviously valid in the two limiting cases where the impurities are far apart or close to each other. If the impurities are far apart the deformations of the CDW due to different impurities are independent from each other. If the impurities are close to each other we suppose that  $X \equiv \tan(\varphi(x)/4)$  is almost constant in the middle of the soliton and if  $l \simeq \xi$  (meaning that  $x\xi \lesssim 1$ ) we use the approximation

$$\tan\left(\frac{\varphi(x)}{4}\right) \simeq X \exp\left(-\frac{|x-\bar{x}|}{\xi}\right), \quad (7)$$

with  $\bar{x} = (\sum_{i=1}^{N_{\text{imp}}} x_i)/N_{\text{imp}}$ . The elastic energy corresponding to the second term of Eq. (1) is independent on

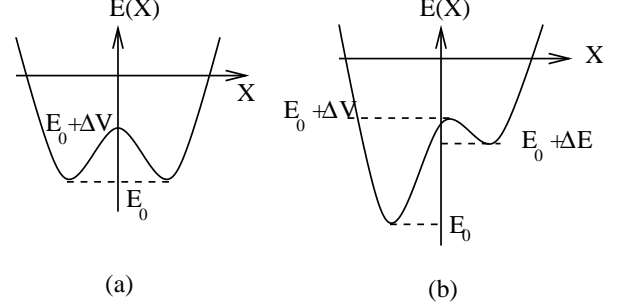


FIG. 2: Schematic representation of the energy landscape in the commensurate case (a) and in the incommensurate case (b). The ground state is at energy  $E_0$ . The metastable state is at energy  $E_0 + \Delta E$ , where  $\Delta E$  is the splitting. The unstable “bounce” state is at energy  $E_0 + \Delta V$  where  $\Delta V$  is the energy barrier.

the number  $N_{\text{imp}}$  of impurities because it arises from the two sides of the soliton profile where  $\partial\varphi(x)/\partial x$  is important. By contrast the pinning energy is additive because each impurity brings its own pinning energy. The additivity property holds if the impurities are within the decay length  $\xi$  so that we work with the model having a binomial distribution of  $N_{\text{imp}}$  in the regime  $x\xi \lesssim 1$ .

The energy landscape generalizing Ref. 13 is given by

$$E(X) = 16w\xi \frac{X^2}{1+X^2} - 2 \sum_{i=1}^{N_{\text{imp}}} V_i \left[ \sin\left(\frac{\alpha_i}{2}\right) \frac{1-X^2}{1+X^2} + \cos\left(\frac{\alpha_i}{2}\right) \frac{2X}{1+X^2} \right]^2, \quad (8)$$

where the elastic and interchain coupling energies in the first term, are much smaller in magnitude than the pinning energy, but will nevertheless play a role in lifting the degeneracy of the effective two level system. Minimizing Eq.(8) in the case of a single impurity leads to the exact solution given by Eq.(3).

In practise we work with an open chain having a width  $\xi$  in the presence of a concentration  $x$  of impurities. The number of impurities fluctuates from one realization of disorder to the other as explained previously. In the incommensurate case with  $\delta Q\xi > 2\pi$  the phases  $\alpha_i$  can be considered as independent random variables (we note  $Q = 2\pi + \delta Q$ , where  $\delta Q$  is the deviation from commensurability).

## B. Properties of the energy landscape

### 1. Distribution of level splittings

The energy landscape  $E(X)$  given by (8) describes a ground state, separated from a metastable state by an energy barrier. There might be more than two energy minima for some realizations of disorder<sup>21,22</sup>. In this case we restrict the energy landscape to the ground state and

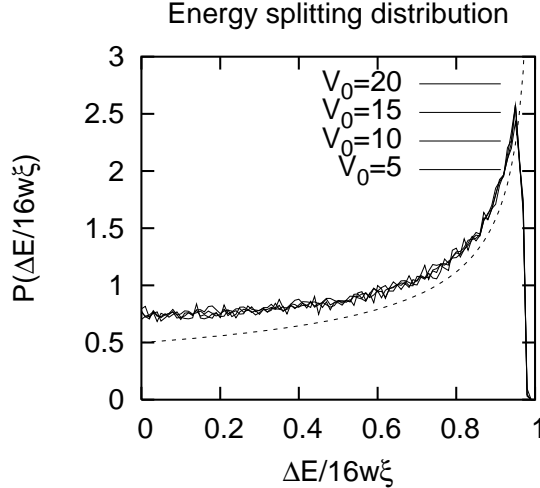


FIG. 3: Distribution of level splitting  $\Delta E$  for the model with random phases discussed in section II A 2. The impurities are distributed at random on a chain of length  $\xi$ . The impurity concentration is such that the average number of impurities is  $\bar{N}_{\text{imp}} = x\xi = 1$ . The curves corresponding to  $x\xi = 0.5$  and  $x\xi = 5$  are superposed on the curves corresponding to  $x\xi = 1$ . The pinning potentials  $V_i$  are uniformly distributed in the interval  $[0, V_0]$  with  $V_0$  indicated on the figure. The distribution of level splitting normalized to  $16w\xi$  is almost independent on  $w\xi$  and  $V_0$ , chosen such that  $16w\xi \ll V_0$ . The dashed line corresponds to  $P(y) = 1/[2\sqrt{1-y}]$ , with  $y = \Delta E/16w\xi$  (see Eq. 9).

to the energy minimum separated from the ground state by the lowest energy barrier. We note  $\Delta E$  the difference between the energies of the metastable state and the ground state and  $\Delta V$  the energy barrier (see Fig. 2). In the dimerized case ( $Q = 2\pi$ ,  $\alpha = 0$ )  $\Delta E$  is equal to zero since the energy landscape is symmetric under a change of sign of the “coordinate”  $X$ . As a consequence it is not possible to communicate energy to the system by increasing temperature except if quantum tunneling is possible. The classical model predicts no slow relaxation at all in the commensurate case whereas in experiments there exists slow relaxation, even though faster than in the incommensurate compound. Adding quantum tunneling between the two energy minima of the energy landscape generates two non degenerate energy levels corresponding to symmetric and antisymmetric wave functions, therefore restoring a finite heat response.

In the incommensurate case we use the model with random phases discussed in section II A 2. The distribution of energy splitting is shown on Fig. 3. The distribution of splitting is close to

$$P\left(\frac{\Delta E}{16w\xi}\right) \simeq \frac{1}{2} \left(1 - \frac{\Delta E}{16w\xi}\right)^{-1/2}, \quad (9)$$

that corresponds to phases such that  $\cos(\alpha/2) \simeq 0$ . The most probable level spacing is close to  $16w\xi$ , independent on the value of the pinning potential and on the number

of impurities involved in the soliton, showing that the shape of  $P(\frac{\Delta E}{16w\xi})$  is almost unchanged when the concentration of impurities increases. The existence of a singularity is in agreement with the experimental observation of a high temperature tail  $C_v \sim 1/T^2$  of a Shottky anomaly in the equilibrium specific heat, with a well-defined level splitting. Experimentally the level splitting  $\Delta E_0$  of a two-level system is related to the temperature  $T_{\text{max}}$  of the maximum of the Shottky anomaly by the relation  $\Delta E_0 \simeq 2.5k_B T_{\text{max}}$ . It was shown experimentally that  $T_{\text{max}} < 30$  mK<sup>9</sup> so that  $\Delta E_0 = 16w\xi \lesssim 100$  mK. The existence of a well-defined level splitting in experiments is a universal property, valid for commensurate and incommensurate systems, and independent on the value of the CDW or SDW critical temperature that can vary by more than one order of magnitude from one compound to the other ( $T_{\text{Peierls}} = 218$  K for o-TaS<sub>3</sub>,  $T_{\text{SDW}} = 12$  K for (TMTSF)<sub>2</sub>PF<sub>6</sub>,  $T_{\text{SP}} = 15$  K for the spin-Peierls compound (TMTTF)<sub>2</sub>PF<sub>6</sub>,  $T_{\text{AF}} = 13$  K for the antiferromagnet (TMTTF)<sub>2</sub>Br). This is compatible with the fact that  $\Delta E_0$  is related only to the strength  $w$  of interchain interactions and the Fermi velocity  $v_F$ :

$$\Delta E_0 = \frac{16}{\sqrt{2\pi}} \sqrt{\hbar v_F w}, \quad (10)$$

where  $v_F$  has the same magnitude for several compounds (for instance  $v_F = 0.86 \times 10^7$  cm.sec<sup>-1</sup> in (TMTSF)<sub>2</sub>PF<sub>6</sub><sup>10</sup>) and interchain couplings are also expected to take similar orders of magnitude, from what we deduce that  $\Delta E_0$  is almost identical in all samples, independent on the charge or spin gap.

## 2. Distribution of energy barriers

We show on Fig. 4 the distribution of energy barriers  $P(\Delta V/V_0)$ . The distributions obtained for different values of  $V_0$  (the upper bound in the pinning energy distribution) and for different values of  $x\xi$  collapse on the same curve

$$\ln \left[ P \left( f(x\xi) \frac{\Delta V}{V_0} \right) \right] \simeq -\alpha - \beta \frac{\Delta V}{V_0} - \gamma \left( \frac{\Delta V}{V_0} \right)^2, \quad (11)$$

if the distribution is plotted as a function of  $f(x\xi)\Delta V/V_0$ . The parameters  $\alpha$ ,  $\beta$ ,  $\gamma$  and the scaling factor  $f(x\xi)$  are determined numerically (see Fig. 4). The discontinuity at  $f(x\xi)\Delta V/\Delta V_0 \simeq 1.7$  is due to an abrupt change in the barrier distribution when going from  $N_{\text{imp}} = 1$  to  $N_{\text{imp}} = 2$ . The transition from  $N_{\text{imp}} = 2$  to  $N_{\text{imp}} = 3$  is much more smooth as seen on Fig. 4.

We found that the scaling form given by Eq.(11) is well obeyed even for values of  $x\xi$  that are artificially large compared to criterion of non proliferation of the solitons (we carried out the same simulation with  $x\xi = 5$  whereas  $x\xi \lesssim 1$  from the non proliferation of solitons – see section II A 2). Without the quadratic term the system would have exactly the weak ergodicity breaking property like in Ref.12 in spite of the difference in the models

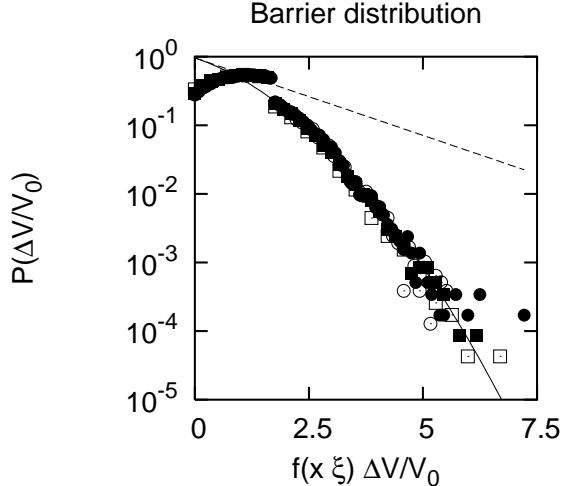


FIG. 4: Distribution of energy barriers  $\Delta V$  for the model with random phases discussed in section II A 2. We use  $\bar{N}_{\text{imp}} = x\xi = 0.5, 1, 1.5$ . The pinning potentials  $V_i$  are uniformly distributed in the interval  $[0, V_0]$  with  $V_0$  indicated on the figure. The distribution of energy barriers is almost independent on  $w\xi$  that is chosen much smaller than  $V_0$ . The solid line corresponds to the fit given by Eq. (11), with  $f(0.5) = 1.2$ ,  $f(1) = 0.95$ ,  $f(1.5) = 0.6$  and  $\alpha = 0.017$ ,  $\beta = 0.226$ ,  $\gamma = 0.077$ . The dashed line corresponds to the same values of  $\alpha$  and  $\beta$  but  $\gamma = 0$ .

(a collection of two-level systems considered here versus a REM-like landscape<sup>12</sup>). Compared to the REM-like trap model of disordered CDWs discussed previously<sup>13</sup> interrupted ageing is due here to the quadratic term in Eq. (11) whereas in Ref. 13 the trap energy distribution was chosen to be exponential up to a maximal energy cut-off  $E_{\text{max}}$ , with no trap energies larger than  $E_{\text{max}}$ .

In the energy landscape  $E(X)$  given by Eq. (8) the pinning energy is roughly proportional to the number of impurities  $N_{\text{imp}}$  so that one can consider a simpler model in which the barrier is given by  $\Delta V = N_{\text{imp}}V_0$ . The distribution of barriers of this simpler model is equal to the distribution of the number of impurities, up to the factor  $V_0$ , and is well described by Eq. (11) in the range  $x\xi = 0.5 \div 1.5$ .

### C. Out-of-equilibrium specific heat

To evaluate energy relaxation in the incommensurate case, we restrict the energy landscape to the ground state, the metastable state and the unstable “bounce” state at the top of the barrier. We are left with a two-state trap model with energies  $-E_1$  and  $-E_2$  (with  $E_1 > E_2$ ).  $E_1$  is equal to the barrier  $\Delta V$  calculated in the preceding section and  $E_2$  is equal to the barrier  $\Delta V$  minus the splitting  $\Delta E$ . The unstable state is at zero energy. We note  $P_1(t)$  ( $P_2(t)$ ) the probability to be in state “1” (“2”) at time  $t$  and note  $\tilde{P}_{1,2}(t) = P_{1,2}(t) \exp(-E_{1,2}/2T)$ . The evolu-

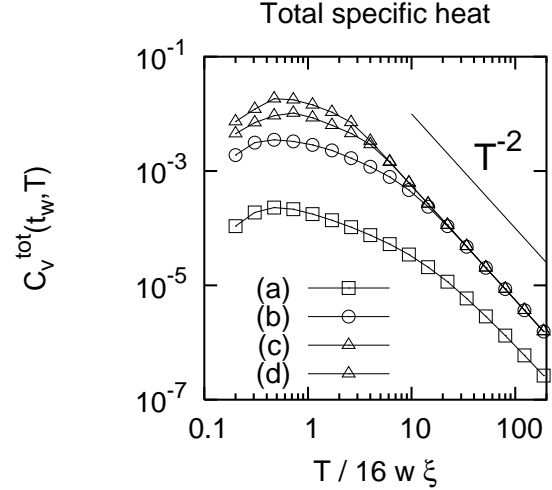


FIG. 5: Variation of the out-of-equilibrium total specific heat as a function of the reduced temperature  $T/16w\xi$ , for different values of  $t_w/\tau_0$ :  $t_w/\tau_0 = 0.1$  (a),  $t_w/\tau_0 = 4.0$  (b),  $t_w/\tau_0 = 1.6 \times 10^2$  (c),  $t_w/\tau_0 = 6.3 \times 10^3$  (d). We used  $x\xi = 1$ . The pinning potentials  $V_i$  are uniformly distributed in the interval  $[0, V_0]$  with  $V_0/16w\xi = 12.5$ . The specific heat for long  $t_w/\tau_0$  follows a  $1/T^2$  behavior for  $T/16w\xi \gtrsim 2$ , where  $16w\xi$  is the maximal splitting. The solid line represents the  $C_v \sim T^{-2}$  behavior.

tion of the probabilities is given by Glauber dynamics<sup>33</sup>

$$\tau_0 \frac{d}{dt} \begin{bmatrix} \tilde{P}_1 \\ \tilde{P}_2 \end{bmatrix} = \hat{G} \begin{bmatrix} \tilde{P}_1 \\ \tilde{P}_2 \end{bmatrix}, \quad (12)$$

with  $G_{1,1} = -\exp(-E_1/T)$ ,  $G_{2,2} = -\exp(-E_2/T)$ ,  $G_{1,2} = G_{2,1} = \exp(-(E_1 + E_2)/2T)$ . Experimentally the time  $\tau_0$  associated to soliton dynamics is of order of 1 sec for the thermally activated process. The time dependence of the occupation probabilities  $P_1(t)$  and  $P_2(t)$  is obtained by diagonalizing the  $2 \times 2$  matrix  $\hat{G}$ , from what we deduce the value of the energy  $U(t_w, t_w + \tau, T)$  as a function of the waiting time  $t_w$ , the time  $\tau$  elapsed since the waiting time and temperature  $T$ . The out-of-equilibrium total specific heat is defined as the total heat released divided by the temperature variation:

$$C_v^{\text{tot}}(t_w, T) = \frac{U(t_w, t_w, T + \Delta T) - U(0, 0, T)}{\Delta T}. \quad (13)$$

The variations of the out-of-equilibrium total specific heat  $C_v^{\text{tot}}(t_w, T)$  as a function of temperature  $T$  for different values of the waiting time  $t_w$  are shown on Fig. 5 for a finite concentration of incommensurate impurities. At temperatures larger than the maximal splitting  $\Delta E = 16w\xi$  the out-of-equilibrium specific heat follows a  $1/T^2$  behavior, in agreement with experiments (see Fig. 3 in Ref. 9). The out-of-equilibrium specific heat is strongly reduced as the waiting time decreases but still follows a  $1/T^2$  behavior, in agreement with experiments<sup>9</sup>.

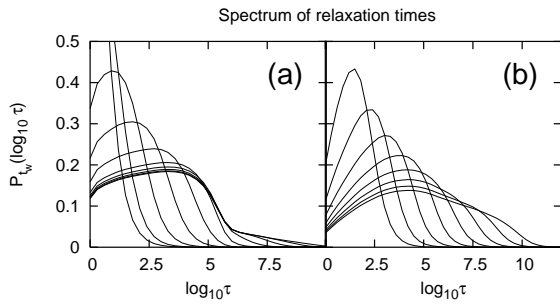


FIG. 6: Spectrum of relaxation times deduced from energy relaxation (see Eq.(14)). We use  $V_0/16w\xi = 2 \times 10^3$ ,  $T/16w\xi = 304$ ,  $T/V_0 = 0.152$ , and  $x\xi = 1$  (a),  $x\xi = 5$  (b). The pinning potentials  $V_i$  are uniformly distributed in the interval  $[0, V_0]$ . The waiting times correspond to  $\log_{10}(t_w/\tau_0) = 2.2, 3.3, 4.4, 5.5, 6.6, 7.7, 8.8, 9.9$ .

#### D. Spectrum of relaxation times

Let  $U(t_w, t_w + \tau, T)$  be the energy of the two-level system at time  $t = t_w + \tau$ , with a heat pulse applied between  $t = 0$  and  $t = t_w$ . The spectrum of relaxation times is deduced from  $U(t_w, t_w + \tau, T)$  by the relation

$$P_{t_w}(\ln \tau) \propto \frac{\partial U(t_w, t_w + \tau, T)}{\partial \ln \tau}, \quad (14)$$

and is afterwards normalized to unity so that  $\int_{-\infty}^{+\infty} P_{t_w}(\ln \tau) d \ln \tau = 1$ . We have shown on Fig. 6 the spectra of relaxation times  $P_{t_w}(\ln \tau)$  for  $x\xi = 1$  and  $x\xi = 5$ . The average value  $\ln \tau = \int d \ln \tau \ln \tau P_{t_w}(\ln \tau)$  and the width of the spectra increase as the waiting time increases. There exists a saturation for long waiting times, in agreement with interrupted ageing for a homogeneous dynamics. The long time tail of the spectrum is a power-law, in agreement with experiments (see Ref. 13). The relaxation time distribution obtained from our model shows homogeneous relaxation and interrupted ageing. The relaxation time spectra corresponding  $x\xi = 5$  are closer to experiments than the spectra corresponding to  $x\xi = 1$  even though solitons are expected to proliferate for  $x\xi = 5$  (see section II A 2).

### III. QUANTUM LIMIT (SUBSTITUTIONAL AND STRONG PINNING IMPURITIES)

We base the discussion in this section on the electronic part of the Peierls Hamiltonian. We discuss a model of disordered CDW but the qualitative results are expected to hold also for SDWs. This is based on the fact that one dimensional tight binding models can be mapped onto XX magnets in one dimension through a Jordan-Wigner transformation. Substitutional disorder in a spin-Peierls system (relevant to  $\text{Cu}_{1-x}\text{Zn}_x\text{GeO}_3$ ) is qualitatively equivalent to impurities that break the chains into finite length segments (see section III C).

There is a flat classical energy landscape in the case of open chains for the model defined by Eq.(1) in the limit  $w = 0$ . The bound state associated to a single impurity in the quantum model is thus at the lowest possible energy (in the middle of the gap). The bound state can be occupied by an electron and a hole with an equal probability, and there is a fast dynamics of the occupation probability since there are no energy barriers in the classical limit. By contrast there is an energy barrier separating two degenerate minima and slow dynamics in the case of strong pinning with  $Q = 2\pi$ , relevant to the organic spin-Peierls compound  $(\text{TMTTF})_2\text{PF}_6$ . In the case of commensurate strong pinning impurities the bound states are away from the Fermi level. The energy of the lowest particle-hole excitation is of order  $\Delta$ , and large energy barriers are expected. This qualitative argument based on quantum effects allows to understand the difference between the spin-Peierls compound  $\text{Cu}_{1-x}\text{Zn}_x\text{GeO}_3$  (with a fast dynamics and antiferromagnetic ordering) and the spin-Peierls compound  $(\text{TMTTF})_2\text{PF}_6$  (with a slow dynamics and no antiferromagnetic ordering).

The width of a soliton in the quantum limit is equal to

$$\xi_0(\omega) = \frac{2\hbar v_F}{\sqrt{\Delta^2 - \omega^2}}, \quad (15)$$

where  $\omega$  is the energy,  $\Delta$  is equal to the Peierls gap and  $v_F$  is the Fermi velocity in the absence of lattice distortions.  $\xi_0$  is different from the soliton width in the classical limit  $\xi = \sqrt{\hbar v_F/2\pi w}$  discussed in the preceding section. In the classical model one should incorporate interchain interactions for the soliton to have a finite width whereas in the quantum model the zero energy soliton width is finite in the absence of interchain interactions. Experimentally the slow relaxation properties associated to the  $1/T^2$  tail of the specific heat are independent on the value of the gap  $\Delta$  and of the transition temperature that can vary by more than one order of magnitude. In the case of the SDW  $(\text{TMTSF})_2\text{PF}_6$  we have the BCS-like relation  $\Delta \simeq 1.7T_c$  is well verified ( $T_c = 11.5 \div 12$  K and  $\Delta = 20$  K from NMR<sup>34</sup>). The Fermi velocity<sup>10</sup> is  $v_F \simeq 0.86 \times 10^7 \text{ cm.sec}^{-1}$  so that  $\xi_0 = 2\hbar v_F/\Delta \simeq 90a_0$ , with the lattice parameter  $a_0 = 7.3 \text{ \AA}$ . In the case of o-TaS<sub>3</sub> we do not have a precise data for  $v_F$  and we take  $v_F = 10^7 \text{ cm.sec}^{-1}$  as a typical value. We have  $T_c^{(\text{CDW})} = 215$  K and  $\Delta_{\text{CDW}} = 3.73T_c \simeq 780$  K so that  $\xi_0^{(\text{CDW})} = 6a_0$  with  $a_0 = 3.34 \text{ \AA}$ . However it is likely that there is also a smaller spin gap since the spin susceptibility follows a power-law. An energy scale  $E = 30$  K can be estimated from the deviations of the power-law. Assuming that the power-law susceptibility is due to randomly distributed magnetic moments we identify the energy scale  $E$  to the average exchange energy  $J_{\text{av}} = \Delta x\xi$  with  $x\xi = 0.3$  estimated from the power-law susceptibility (see section III C 2) so that  $\xi_0^{(\text{spin})} = 150 \div 450a_0$ .  $\xi_0^{(\text{spin})}$  in the SDW compound  $(\text{TMTSF})_2\text{PF}_6$  and o-TaS<sub>3</sub> are thus one order of magnitude larger than  $\xi_0$  in the spin-Peierls compound CuGeO<sub>3</sub>.

### A. Hamiltonian

We use the Peierls Hamiltonian for charge degrees of freedom, the electronic part of which is given by

$$\mathcal{H} = \sum_i [t + \epsilon \cos(2k_F x_i)] [c_{i+1}^+ c_i + c_i^+ c_{i+1}], \quad (16)$$

where spinless fermions jump between neighboring sites on a 1D chain. We suppose that the lattice is frozen and therefore we do not include in the Hamiltonian the term due to the lattice deformations.  $t$  in Eq. (16) is equal to the average hopping amplitude and  $\epsilon$  is the amplitude of the modulation. The variable  $x_i$  in Eq.(16) is the coordinate of the site number  $i$ :  $x_i = ia_0$ , with  $a_0$  the lattice parameter. The Hamiltonian (16) is diagonal in terms of the operators  $\gamma_{k,R}$  and  $\gamma_{k,L}$ , where R and L label right and left-moving fermions:

$$\mathcal{H} = \sum_k [E_{k,R} \gamma_{k,R}^+ \gamma_{k,R} + E_{k,L} \gamma_{k,L}^+ \gamma_{k,L}], \quad (17)$$

with

$$\gamma_{k,R}^+ = \mathcal{N}_k^{(R)} [c_{k,R}^+ + \mathcal{B}_k^{(R)} c_{k-2k_F,L}^+] \quad (18)$$

$$\gamma_{k,L}^+ = \mathcal{N}_k^{(L)} [c_{k,L}^+ + \mathcal{B}_k^{(L)} c_{k+2k_F,R}^+], \quad (19)$$

and

$$E_{k,R} = 2t \cos(ka_0) - \frac{\epsilon^2}{4t \sin(k_F a_0)} \frac{1}{(k - k_F)a_0} \quad (20)$$

$$E_{k,L} = 2t \cos(ka_0) + \frac{\epsilon^2}{4t \sin(k_F a_0)} \frac{1}{(k + k_F)a_0}. \quad (21)$$

The coefficients  $\mathcal{B}_k^{(R)}$  and  $\mathcal{B}_k^{(L)}$  are given by

$$\mathcal{B}_k^{(R)} = -\frac{\epsilon \exp(ik_F a_0)}{4t (k - k_F)a_0} \quad (22)$$

$$\mathcal{B}_k^{(L)} = \frac{\epsilon \exp(-ik_F a_0)}{4t (k + k_F)a_0}. \quad (23)$$

The normalization coefficients are given by  $\mathcal{N}_k^{(R,L)} = 1/\sqrt{1 + |\mathcal{B}_k^{(R,L)}|^2}$ . The Green's functions deduced from the spectral representations are given in Appendix A.

### B. Strong pinning impurities

#### 1. Dyson matrix

The Hamiltonian is equal to (16), plus a term describing the impurities:

$$H_{\text{imp}} = - \sum_i V_{y_i} c_{y_i}^+ c_{y_i}, \quad (24)$$

where the strong pinning impurities are located at random positions  $\{y_1, \dots, y_{N_{\text{imp}}}\}$ . We suppose that  $V_{y_i} = V$

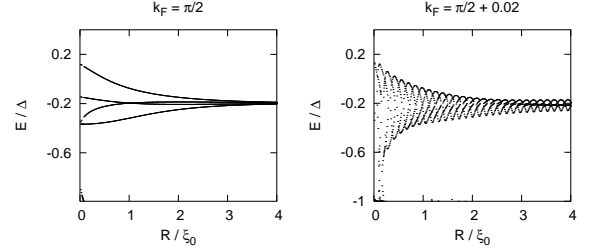


FIG. 7: Evolution of the bound state energy levels as a function of the distance between the two pinning centers, in the commensurate case  $k_F = \pi/2$  (a) and in the incommensurate case  $k_F = \pi/2 + \delta k_F$ , with  $\delta k_F = 0.02$  (b). The energy is in units of  $\Delta = \sqrt{2}\epsilon$  and the distance is in units of  $\xi_0 = 2v_F/\Delta$ . We used  $\epsilon/t = 10^{-3}$  and  $V/t = 10$ .

is the same for all impurities and that  $V > 0$ . We note  $G(\omega)$  the Green's function in the presence of the pinning potential and  $g(\omega)$  the Green's function in the absence of pinning potential. The Green's function  $G(\omega)$  is obtained from inverting the Dyson matrix:

$$\sum_{k=1}^{N_{\text{imp}}} [\delta_{i,k} + g_{x_i, x_k}(\omega) V_{x_k}] G_{x_k, x_j}(\omega) = g_{x_i, x_j}(\omega), \quad (25)$$

where the Green's function  $g_{x_i, x_k}(\omega)$  is given in Appendix A. The bound state energies correspond to the poles of  $G(\omega)$ .

#### 2. Two pinning centers

In the commensurate case  $k_F a_0 = \pi/2$  the energy levels evolve smoothly as a function of the distance between the two impurities (see Fig. 7-(a)). In the incommensurate case  $k_F a_0 = \pi/2 + \delta k_F$  (see Fig. 7-(b)) the energy levels fluctuate strongly as the distance between the two impurities is reduced. This shows that quantum mechanical interactions among impurities enhance disorder effects in the incommensurate case but not in the commensurate case.

### C. Substitutional disorder

#### 1. Open chains in the dimerized limit

Let us consider two semi-infinite dimerized chains ending at sites "a" and "α" (see Fig. 8-(a)). We note  $t_0 = t_{a,\alpha}$  the value of the hopping between sites "a" and "α" (equal to  $t + \epsilon$  or  $t - \epsilon$ ) in the infinite chain. The Dyson equation relates the Green's functions  $g_{i,j}$  of the infinite chain to the Green's functions  $G_{i,j}$  of the semi-infinite chain:

$$g_{a,a}(\omega) = G_{a,a}(\omega) + t_0^2 G_{a,a}(\omega) g_{a,a}(\omega) \quad (26)$$

$$g_{\alpha,\alpha}(\omega) = G_{\alpha,\alpha}(\omega) + t_0^2 G_{\alpha,\alpha}(\omega) g_{\alpha,\alpha}(\omega), \quad (27)$$

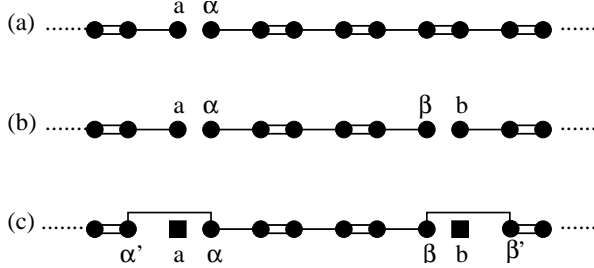


FIG. 8: Schematic representation of a dimerized CDW chains with open boundary conditions with one impurity (a) or two impurities (b). The double lines represent the strong bonds  $t + \epsilon$ . (b) corresponds to  $R = x_\beta - x_\alpha$  odd. We represented on (c) two substitutional impurities (black square) leaving unpaired fermions at sites  $\alpha$  and  $\beta$ .

with  $g_{a,a} = g_{\alpha,\alpha} = \omega/(2t\sqrt{2\epsilon^2 - \omega^2})$ . The solution of (26) and (27) is

$$G_{a,a} = \frac{t}{t_0^2} \frac{\sqrt{2\epsilon^2 - \omega^2}}{\omega} \left\{ -1 + \eta_a \sqrt{1 + \frac{t_0^2}{t^2} \frac{\omega^2}{2\epsilon^2 - \omega^2}} \right\}, \quad (28)$$

with  $\eta_a = \pm 1$ . In the case of two weak bonds in the chain (see Fig. 8-(b)) we find  $G_{\alpha,\beta} = g_{\alpha,\beta}/\mathcal{D}$ , with

$$\mathcal{D} = [1 + t_{a,\alpha}^2 G_{a,a} g_{\alpha,\alpha}] [1 + t_{b,\beta}^2 G_{b,b} g_{\beta,\beta}] - t_{a,\alpha}^2 t_{b,\beta}^2 G_{a,a} G_{b,b} g_{\alpha,\beta} g_{\beta,\alpha}. \quad (29)$$

If the separation between the boundaries is large enough the energy of the bound states can be expanded in the small parameter  $\exp(-R/\xi_0)$  where  $\xi_0/a_0 = 2\sqrt{2}t/\epsilon$  is the zero energy coherence length. Since the bound states are close to the Fermi energy we also expand  $G_{\alpha,\beta}$  in powers of  $\omega$ . If  $R = x_\beta - x_\alpha$  is even we find that one bound state is generated at one end of the chain. In the case  $R$  odd on Fig. 8-(b) we find two bound states at  $\omega^{(\pm)} = \pm(\epsilon/3) \exp(-R/\xi_0)$  corresponding to  $\eta_a = \eta_b = -1$ . In the ground state  $\omega^{(-)}$  is occupied with an electron and  $\omega^{(+)}$  is occupied with a hole. The lowest neutral excitation corresponds to an electron in the level  $\omega^{(+)}$  and a hole in the level  $\omega^{(-)}$ . This is in agreement with a previous model developed for the spin-Peierls compound  $\text{Cu}_{1-x}\text{Zn}_x\text{O}_3$ <sup>32</sup> as well as in a qualitative agreement with numerical simulations<sup>35,36</sup>.

## 2. Substitutional disorder in CDWs and SDWs

We consider now a more realistic model of substitutional disorder, both for commensurate and incommensurate CDWs. We suppose that two substitutional impurities “remove” the sites “a” and “b” from the chain and that second neighbor interactions  $t_{\alpha,\alpha'}$  and  $t_{\beta,\beta'}$  couple the right and left neighbors (see Fig. 8-(c)). The model is similar to Ref. 32 proposed for Zn impurities in  $\text{CuGeO}_3$  except that we consider here the incommensurate case.

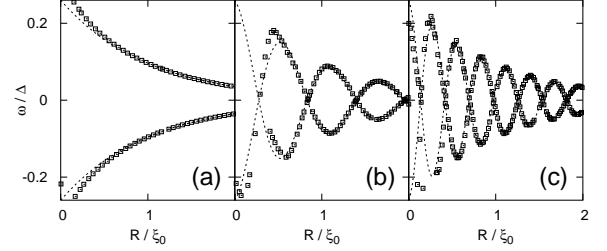


FIG. 9: Evolution of the bound state energies as a function of the distance  $R = |x_a - x_b|$  between the two impurities. We use  $k_F = \pi/2 + \delta k_F$ , with  $\delta k_F = 0$  (a),  $\delta k_F = 0.02$  (b) and  $\delta k_F = 0.04$  (c). We use the parameters  $\epsilon/t = 10^{-2}$ .  $t_{\alpha,\alpha'}/t = t_{\beta,\beta'}/t = 1/2$ . The dashed line is a fit to  $\omega/\Delta = \pm 0.26 \cos((\delta k_F)R) \exp(-R/\xi_0)$ .

We calculate the poles and residues as a function of the distance  $R = |x_a - x_b|$  between the two impurities (see Fig. 9). We use  $k_F = k_F^{(0)} + \delta k_F$ , with  $k_F^{(0)} = \pi/2$  and show on Fig. 9 the Friedel oscillations of the bound state levels for odd values of  $R$ . The phase of the Friedel oscillations is shifted by  $\pi/2$  for even values of  $R$ . We deduce from the level crossings that there exists a change of sign in the hopping amplitude between the two solitons as  $R$  is increased. Substitutional disorder in incommensurate systems leads therefore to frustration if  $\delta k_F \xi_0 > 2\pi$  and possible 3D glasses in CDWs or spin glasses in SDWs if interchain interactions are large enough<sup>37</sup>.

Similarly to a model of doped spin-Peierls system<sup>32</sup> substitutional disorder in CDWs and SDWs provides an explanation to the power-law specific heat  $C_v \sim T^\alpha$  observed in disordered CDWs and SDWs, and to the susceptibility  $\chi(T) \sim T^{-1+\alpha}$  observed in the CDW o-TaS<sub>3</sub><sup>26</sup> (with the same value of  $\alpha$  in the specific heat and susceptibility experiments). In experiments on the SDW (TMTSF)<sub>2</sub>PF<sub>6</sub><sup>11</sup>, on changing the time constant in a heat pulse experiment by a factor of 100, there is an increase by a factor of 7 of the amplitude of the  $T^{-2}$  contribution whereas the  $T^\alpha$  contribution changes only by 20%, and not in a systematic manner. In the commensurate (TMTTF)<sub>2</sub>Br compound and also in a heat pulse experiment, an increase of the time constant by a factor of 3 results in an increase of the  $T^{-2}$  term by a factor of 3 and only an increase of the  $T^\alpha$  term by 20%. This shows that the  $T^\alpha$  contribution to the specific heat can be interpreted as an equilibrium property, which is the case if frustration due to Friedel oscillations can be neglected as in a dilute one dimensional model. In this case we consider only exchanges  $J(R)$  between nearest neighbor solitons and disregard the changes of sign in  $J(R)$ . The exchange distribution scales like  $P(|J|) \sim |J|^{-1+x\xi_0}$ , where  $x$  is the concentration of substitutional impurities<sup>32</sup>. The energy of “active” pairs of spins is approximately given by  $U = \int_0^T JP(J)dJ$ , where  $T$  is the temperature so that the temperature dependence of the specific heat is given by  $C_v \sim T^{x\xi_0}$ . The susceptibility is approximately given by a Curie contribution for the fraction of “active” spin

having an energy smaller than  $T$  so that the susceptibility behaves like  $\chi(T) \sim T^{-1+x\xi_0}$ , leading to  $\alpha = x\xi_0$ . Experimentally  $\alpha = 0.3 \div 1.2$  as mentioned in the Introduction. In the case of o-TaS<sub>3</sub> we estimate  $\xi_0 \simeq 150 \div 450 a_0$  in the spin sector as mentioned previously and  $\alpha = 0.3$  obtained from specific heat and susceptibility. We deduce the concentration of intrinsic substitutional impurities  $x_{\text{int}} \simeq 0.07 \div 0.2\%$ . The upper bound is comparable to the nominal concentration of extrinsic Nb impurities  $x_{\text{ext}} \simeq 0.5\%$  which might explain why the exponent  $\alpha$  in the experiment is the same in the presence or absence of extrinsic impurities.

#### IV. CONCLUSIONS

To conclude we have investigated several factors involved in energy relaxation in disordered CDWs and SDWs. A first factor is the role of commensuration. In the commensurate case we find that the energy landscape is symmetric, so that the two energy minima are degenerate. The symmetry property holds for an arbitrary number of impurities contributing to pinning the soliton. Experimentally there exists heterogeneous slow relaxation in commensurate systems with a bimodal spectrum of relaxation times as opposed to homogeneous relaxation with a broad spectrum in the incommensurate case. The fully classical model might be too schematic since the exact degeneracy of the classical model is lifted by quantum tunneling. In the incommensurate case we find that the distribution of energy splittings  $\Delta E$  (the difference between the energies of the metastable and ground states) shows a peak at approximately  $\Delta E = 16w\xi$ , with  $w$  the interchain coupling and  $\xi$  the width of the soliton. This peak is almost independent on the number of impurities involved in the soliton and generates a well-defined high temperature tail  $C_v \sim 1/T^2$  in the total out-of-equilibrium specific heat, in agreement with experiments on incommensurate compounds. The commensurate compounds also show experimentally a well-defined energy level splitting even though the classical energy landscape is degenerate.

Finally we discussed another important factor: the nature of disorder at the level of a single soliton and the possibility of quantum interactions among solitons that might explain the differences between the spin-Peierls compound Cu<sub>1-x</sub>Zn<sub>x</sub>GeO<sub>3</sub> that does not show slow relaxation and orders antiferromagnetically, and the spin-Peierls compound (TMTTF)<sub>2</sub>PF<sub>6</sub> that shows slow relaxation without antiferromagnetic order. The energy spectrum of a single quantum mechanical soliton generated by a strong pinning impurity is constant as the position of the soliton varies along the chain in the commensurate case, whereas it varies in the incommensurate case. Interactions among solitons enhance disorder effects in the incommensurate case. We thus find a qualitative difference between the commensurate and incommensurate cases in the quantum limit, that is apparently qualita-

tively compatible with the existence of a heterogeneous versus homogeneous relaxation. A more detailed discussion can be found elsewhere<sup>27</sup>.

For substitutional disorder in the quantum limit we find interactions among solitons due to Friedel oscillations. This can explain the experimentally observed power-law contribution to the specific heat in inorganic CDWs and SDWs in the limit of weak interchain couplings.

The final picture for organic SDWs and CDWs is a co-existence between strong pinning and substitutional disorder as well as a coexistence between classical and quantum effects. Further investigations would require a model of collective effects interpolating between the classical and quantum limits. Another ingredient that we did not discuss in detail is metallic island formed around impurities<sup>38</sup> that would lead to a phenomenology close to that of substitutional disorder because both generate states at the Fermi level for an isolated impurity, that can interact through Friedel oscillations.

#### Acknowledgements

The authors acknowledge fruitful discussions with P. Monceau. K.B. acknowledges funding by CNRS through a temporary position of associate researcher.

#### APPENDIX A: GREEN'S FUNCTIONS OF A CHARGE DENSITY WAVE

The advanced Green's function defined as  $g_{x,y}(t, t') = -i\theta(t-t')\langle\{c_x(t), c_y(t')\}\rangle$  decomposes into the sum of the four right (R) and left (L) combinations:

$$g_{x,y}(t, t') = g_{x,y}^{R,R}(t, t') + g_{x,y}^{R,L}(t, t') + g_{x,y}^{L,R}(t, t') + g_{x,y}^{L,L}(t, t'), \quad (\text{A1})$$

where the "RR" Green's function is defined by

$$g_{x,y}^{R,R}(t, t') = \sum_{k, k'} e^{ikx} e^{-ik'y} \langle\{c_{k,R}(t), c_{k',R}(t')\}\rangle, \quad (\text{A2})$$

and similar expressions are obtained for the "RL", "LR" and "LL" Green's functions. The spectral representation of  $g_{x,y}^{R,R}$  is given by

$$g_{x,y}^{R,R}(\omega) = \sum_k \left[ \mathcal{N}_k^{(R)} \right]^2 e^{ik(x-y)} \quad (\text{A3})$$

$$\times \left\{ \frac{1}{\omega - E_{k,R}} + \frac{|\mathcal{B}_k^{(R)}|^2}{\omega - E_{k-2k_F,L}} \right\}, \quad (\text{A4})$$

and similar expressions are obtained for the three other Green's functions. After performing the integral over wave vector in the spectral representations we obtain

$$g_{x,y}^{R,R}(\omega) + g_{x,y}^{L,L}(\omega) = \frac{2}{3} \frac{1}{2t \sin k_F} \frac{\sqrt{2}\epsilon}{\sqrt{2\epsilon^2 - \omega^2}} \quad (\text{A5})$$

$$\begin{aligned}
& \sin \left\{ \varphi + \left[ k_F - \frac{\omega}{4t \sin k_F} \right] R \right\} \exp(-R/\xi(\omega)) \\
& + \frac{1}{3} \frac{1}{2t \sin k_F} \frac{\sqrt{2}\epsilon}{\sqrt{2\epsilon^2 - \omega^2}} \\
& \sin \left\{ \varphi - \left[ k_F + \frac{\omega}{4t \sin(k_F a_0)} \right] R \right\} \exp(-R/\xi(\omega)),
\end{aligned}$$

$$\begin{aligned}
& - \frac{\sqrt{2}}{3} \frac{1}{2t \sin(k_F a_0)} \frac{\sqrt{2}\epsilon}{\sqrt{2\epsilon^2 - \omega^2}} \exp(-R/\xi(\omega)) \\
& \left\{ \cos \left[ k_F + 2\varphi + \left[ k_F - \frac{\omega}{4t \sin(k_F a_0)} \right] R - 2k_F x \right] \right. \\
& \left. - \cos \left[ k_F - \left[ k_F - \frac{\omega}{4t \sin(k_F a_0)} \right] R - 2k_F y \right] \right\}.
\end{aligned}$$

where  $R = x - y$  is positive and  $\xi(\omega) = 4t \sin(k_F a_0) / \sqrt{2\epsilon^2 - \omega^2}$  is the coherence length at a finite frequency. The sum of the “RL” and “LR” Green’s functions is given by

$$g_{x,y}^{R,L}(\omega) + g_{x,y}^{L,R}(\omega) = \quad (A6)$$

We obtain similar expressions for  $R < 0$ .

---

<sup>1</sup> L. Lundgren, P. Svedlindh, P. Nordblad and O. Beckmann, Phys. Rev. Lett. **51**, 911 (1983); P. Nordblad, L. Lundgren, P. Svedlindh and L. Sandlund, Phys. Rev. B **33**, 645 (1988).

<sup>2</sup> V. Dupuis, E. Vincent, J.P. Bouchaud, J. Hammam, A. Ito, and H. Aruga Katori, cond-mat/0104399; K. Jonason, E. Vincent, J. Hammam, J.P. Bouchaud, and P. Nordblad, Phys. Rev. Lett. **81**, 3243 (1998); K. Jonason, P. Nordblad, E. Vincent, J. Hammam, and J.P. Bouchaud, Eur. Phys. Jour. B **13**, 99 (2000).

<sup>3</sup> J. Gilchrist, Phys. Lett. A **156**, 76 (1989), J. of Mol. Liq. **69**, 253 (1996).

<sup>4</sup> F. Alberici, P. Doussineau and A. Levelut, J. Phys. I (France) **7**, 329 (1997); F. Alberici, P. Doussineau and A. Levelut, Europhys. Lett. **39**, 329 (1997).

<sup>5</sup> F. Alberici-Kious, J.P. Bouchaud, L.F. Cugliandolo, P. Doussineau and A. Levelut, Phys. Rev. Lett. **81**, 4987 (1998); F. Alberici-Kious, J.P. Bouchaud, L. F. Cugliandolo, P. Doussineau and A. Levelut, Phys. Rev. B **62**, 14766 (2000).

<sup>6</sup> R.L. Leheny and S. Nagel, Phys. Rev. B **57**, 5154 (1998).

<sup>7</sup> J.C. Lasjaunias, K. Biljaković, D. Staresinic, P. Monceau, S. Takasaki, J. Yamada, S. Nakatsuji, and H. Anzai, Eur. Phys. J. B **7**, 541 (1999).

<sup>8</sup> K. Biljaković, J.C. Lasjaunias, P. Monceau and F. Levy, Phys. Rev. Lett. **62**, 1512 (1989); K. Biljaković, J.C. Lasjaunias, P. Monceau and F. Levy, Phys. Rev. Lett. **67**, 1902 (1991).

<sup>9</sup> J.C. Lasjaunias, J.P. Brison, P. Monceau, D. Staresinic, K. Biljaković, C. Carcel and J. M. Fabre, J. Phys.: Condens. Matter **14** 837 (2002).

<sup>10</sup> G. Grüner, *Density waves in Solids*, Frontiers in Physics, vol. 89 (1994).

<sup>11</sup> K. Biljaković, F. Nad, J.C. Lasjaunias, P. Monceau, and K. Bechgaard, J. Phys. Condens. Matter **6**, L135 (1994); K. Biljaković, F. Nad, J.C. Lasjaunias, P. Monceau, and K. Bechgaard, Synthetic Metals **71**, 1849 (1995); J.C. Lasjaunias, K. Biljaković, and P. Monceau, Phys. Rev. B **53**, 7699 (1996); J.C. Lasjaunias, S. Sahling, K. Biljaković, and P. Monceau, J. of low T. Phys. **130**, 25 (2003).

<sup>12</sup> J.P. Bouchaud, J. Phys. I France **2**, 1705 (1992); J.P. Bouchaud, E. Vincent, and J. Hammam, J. Phys. I France **4**, 139 (1994); J.P. Bouchaud and D.S. Dean, J. Phys. I France **5**, 265 (1995). C. Monthus and J.P. Bouchaud, J. Phys. A **29**, 3847 (1996).

<sup>13</sup> R. Mélin, K. Biljaković, J.C. Lasjaunias and P. Monceau, Eur. Phys. J. B **26**, 417 (2002).

<sup>14</sup> S.K. Ma, C. Dasgupta and C.-K. Hu, Phys. Rev. Lett. **43**, 1434 (1979); C. Dasgupta and S.K. Ma, Phys. Rev. B **22**, 1305 (1980).

<sup>15</sup> D.S. Fisher, P. Le Doussal and C. Monthus, Phys. Rev. Lett. **80**, 3539 (1998); D.S. Fisher, P. Le Doussal and C. Monthus, Phys. Rev. E **64**, 066107 (2001).

<sup>16</sup> H. Fukuyama, J. Phys. Soc. Jpn. **41**, 513 (1976); H. Fukuyama and P. A. Lee, Phys. Rev. B **17**, 535 (1977); P. A. Lee and T. M. Rice, Phys. Rev. B **19**, 3970 (1979).

<sup>17</sup> K. Efetov and A.I. Larkin, Zh. Eksp. Teor. Fiz. **72**, 2350 (1977) [Sov. Phys. JETP **45**, 1236 (1977)].

<sup>18</sup> A.I. Larkin and P. Lee, Phys. Rev. B **17**, 1596 (1978).

<sup>19</sup> P.B. Littlewood and R. Rammal, Phys. Rev. B **38**, 2675 (1988).

<sup>20</sup> S. Brazovskii, *Charge Density waves*, edited by L. Gorkov and G. Grüner (Elsevier, Amsterdam) (1990).

<sup>21</sup> A.I. Larkin, Zh. Eksp. Teor. Fiz. **105**, 1793 (1994); A.I. Larkin Sov. Phys. JETP **78**, 971 (1994).

<sup>22</sup> Yu. N. Ovchinnikov, K. Biljakovic, J.C. Lasjaunias, and P. Monceau, Europhysics Letters **34**, 645 (1996).

<sup>23</sup> S. Brazovskii and T. Nattermann, cond-mat/0312375, Advances in Physics in press (2004).

<sup>24</sup> B. Derrida, Phys. Rev. B **24**, 2613 (1981); B. Derrida and G. Toulouse, J. Phys. Lett. **46**, L223 (1985).

<sup>25</sup> S. Ravy, J.P. Pouget and R. Comes, J. Phys. I France **2**, 1173 (1992); S. Rouzière, S. Ravy, J.P. Pouget and S. Brazovskii, Phys. Rev. B **62**, R16232 (2000); J.P. Pouget, S. Ravy, S. Rouzière and S. Brazovskii, J. Phys. IV France **12**, Pr9-9 (2002); S. Ravy, S. Rouzière, E. Elkaïm, J.P. Pouget and S. Brazovskii, *ibid* **12**, Pr9-79 (2002).

<sup>26</sup> K. Biljakovic, M. Miljak, D. Staresinic, J. C. Lasjaunias, P. Monceau, H. Berger and F. Levy, Eurphys. Lett. **62**, 554 (2003).

<sup>27</sup> J.C. Lasjaunias, R. Mélin, D. Starešinić, K. Biljaković and J. Souletie, submitted to Phys. Rev. Lett.

<sup>28</sup> M. Hase, K. Uchinokura, R.J. Birgeneau, K. Hirota and G. Shirane, J. Phys. Soc. Jpn. **65**, 1392 (1996); M. Hase, N. Koide, K. Manabe, Y. Sasago, K. Uchinokura and A. Sawa, Physica B **215**, 164 (1995).

<sup>29</sup> M.C. Martin, M. Hase, K. Hirota and G. Shirane, Phys.

Rev. B **56**, 3173 (1997).

<sup>30</sup> T. Masuda, A. Fujioka, Y. Uchiyama, I. Tsukada, and K. Uchinokura, Phys. Rev. Lett. **80**, 4566 (1998).

<sup>31</sup> K. Manabe, H. Ishimoto, N. Koide, Y. Sasago, and K. Uchinokura, Phys. Rev. B **58**, R575 (1998).

<sup>32</sup> M. Fabrizio and R. Mélin, Phys. Rev. Lett. **78**, 3382 (1997); M. Fabrizio and R. Mélin, Phys. Rev. B **56**, 5996 (1997); M. Fabrizio, R. Mélin and J. Souletie, Eur. Phys. J. B **10**, 607 (1999); R. Mélin, Eur. Phys. J. B **16**, 261 (2000); R. Mélin, Eur. Phys. J. B **18**, 263 (2000).

<sup>33</sup> R.J. Glauber, Jour. Math. Phys. **4**, 294 (1963).

<sup>34</sup> F. Nad, P. Monceau and K. Bechgaard, Solid State Commun. **95**, 655 (1995), and references therein.

<sup>35</sup> M. Laukamp, G.B. Martins, C. Gazza, A.L. Malvezzi, E. Dagotto, P.M. Hansen, A.C. Lopez and J. Riera, Phys. Rev. B **57**, 10755 (1998).

<sup>36</sup> D. Augier, E. Sørensen, J. Riera, and D. Poilblanc Phys. Rev. B **60**, 1075 (1999); A. Dobry, P. Hansen, J. Riera, D. Augier, and D. Poilblanc, Phys. Rev. B **60**, 4065 (1999); E. Sørensen, I. Affleck, D. Augier, and D. Poilblanc, Phys. Rev. B **58**, R14701 (1998).

<sup>37</sup> R. Mélin *et al.*, in preparation.

<sup>38</sup> S.N. Artemenko and F. Gleisberg, Phys. Rev. Lett. **75**, 497 (1995).